Low Percolation Threshold in Nanocomposites Based on Oxidized Single Wall Carbon Nanotubes and Poly(butylene terephthalate)

A. Nogales,[†] G. Broza,[‡] Z. Roslaniec,[§] K. Schulte,[‡] I. Šics,[⊥] B. S. Hsiao,[⊥] A. Sanz,[†] M. C. García-Gutiérrez,[†] D. R. Rueda,[†] C. Domingo,[†] and T. A. Ezquerra*[,†]

Instituto de Estructura de la Materia, CSIC, Serrano 119, 28006 Madrid, Spain; Technische Universität Hamburg−Harburg, Denickestrasse 15, D-21071 Hamburg, Germany; Institute of Materials Science and Engineering, Technical University of Szczecin, Piastow Av. 19, PL-70310 Szczecin, Poland; and Department of Chemistry, State University of New York at Stony Brook, Stony Brook, New York 11794-3400

Received March 22, 2004; Revised Manuscript Received June 23, 2004

ABSTRACT: To achieve low percolation thresholds in single wall carbon nanotube (SWCNT) and thermoplastic poly(butylene terephthalate) (PBT) composites, we have used an in situ polycondensation reaction process. The intense dispersion process achieved first by ultrasonication and followed by ultrahigh speed stirring of single wall nanotubes in 1,4-butanediol and the subsequent in situ polycondensation has made possible the preparation of nanocomposites in which the percolation threshold is around 0.2 wt % of SWCNT. This relatively low value approaches those reported for carbon nanotube nanocomposites based on thermoset polymers. On the basis of the structural measurements, we interpret that agglomeration effects may enhance the formation of the conducting network.

1. Introduction

Electrical properties of composite materials based on conducting particles dispersed in an insulating polymeric matrix have been intensively studied in the past two decades.[1−3] The electrical properties of the composite may vary from those of an insulating material to those of a conducting system depending on the concentration and on the property of the conducting additives. The effect can be explained by the formation of a percolative path of the conducting network through the sample for a concentration corresponding to the percolation threshold.[1−4] One important technological goal is to achieve the lowest possible percolation threshold in order to reduce the density of the conducting composite and to retain its original mechanical properties. The most studied conductive composites are the system containing carbon black.[1−7] Recently, polymer composites based on carbon nanotubes (CNT) have begun to receive a great deal of attention because of the unique electrical property of CNT.[8−11] The small size and the high aspect ratio of CNT enable electrical percolation at very low loadings, which offers new opportunities to enhance the electrical conductivity at a very low additive concentration. In addition, the presence of CNT also may improve mechanical properties, when compared with the conventional composites containing carbon black.[8−12]

The dispersion of the CNT additive in the insulating matrix is a crucial controlling factor of the final electrical properties.[9] Low percolation thresholds in the 10^{-3}−10^{-1} range of weight % (wt %) of CNT have been reported in multiwall CNT−thermoset composites[9,11] where an extensive dispersion of the additive was achieved before the curing of the resin. However, higher percolation thresholds have been observed when CNT are dispersed in a thermoplastic polymer[10,13] unless the sample thickness was reduced to the nanometer range.[8] This is because the inherently high viscosity of the polymer material often hinders the dispersion of the additives. The objective of this work is to demonstrate that low percolation thresholds could be obtained in a nanocomposite system containing CNT and thermoplastic polyester, poly(butylene terephthalate) (PBT), using an in situ polycondensation reaction process.

2. Experimental Section

For this study several nanocomposite samples of poly(butylene terephthalate) (PBT) with different amounts of oxidized single wall carbon nanotubes (SWCNT) (from CNI Technology Co., Houston, TX, synthesized by using the HIPCO method) were prepared. The diameter of the SWCNT's was characterized through their Raman spectra taken in the backscattering geometry. A Renishaw Raman microscope system RM2000 was used equipped with a Leica microscope, an electrically refrigerated CCD camera, and a diode laser at 785 nm as exciting source. The low-frequency Raman spectrum of our SWNT's is shown in Figure 1. The Raman bands correspond to the low-frequency radial breathing modes (RBM) associated with collective radial movement of the carbon atoms.[14] From the position of the RBM's the diameter, d, of the SWCNT's can be calculated[14] by means of d (nm) = 248/ν (cm^{-1}). The spectrum shows that the investigated SWCNT's consist of different diameter populations ranging from about 0.6 to 1.4 nm. The oxidation process is accomplished in order to remove rest of amorphous carbon and other impurities. The sample preparation scheme was as follows. An appropriate amount of additive was first dispersed in 1,4-butanediol (BASF, Germany) by ultrasonication and followed by ultrahigh speed stirring. The maximum amount of SWCNT that can be added is controlled by the increment in the viscosity of the mixture. In our case this was restricted to 0.2 wt %. Polycondensation was then accomplished by transesterification with dimethyl terephthalate (Elana S.A., Torun, Poland) carried out in an acid resistance steel reactor of 1 L (Autoclave Eng. Inc.) at 150−190 °C. The nanocomposite was extruded from the reactor by compressed nitrogen, and subsequently it was pelletized and injection-molded with a Baby Plast model 6/10 (Cronoplast S.L. Comp) injection molding machine into long pieces with a rectangular cross section of 2 × 4 mm^2. The

[†] Instituto de Estructura de la Materia, CSIC.
[‡] Technische Universität Hamburg−Harburg.
[§] Technical University of Szczecin.
[⊥] State University of New York at Stony Brook.

10.1021/ma049440r CCC: $27.50
Published on Web 08/31/2004

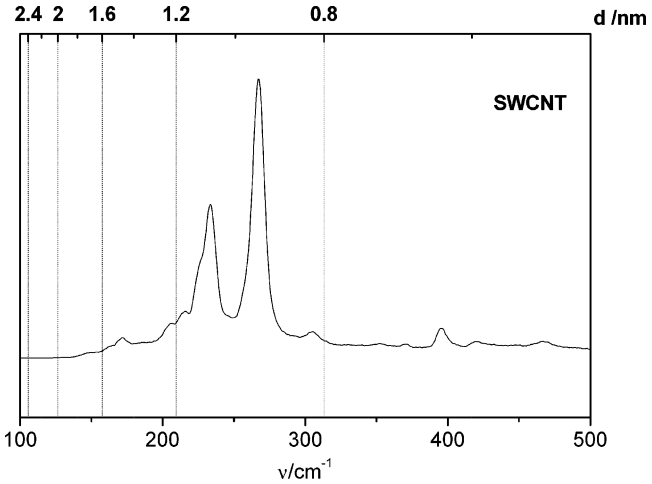

Figure 1. Low-frequency Raman spectrum of SWCNT's showing bands corresponding to the radial breathing modes (RBM). Upper horizontal scale: diameter (nm) according[14] to $248/\nu$ (cm^{-1}). Experimental conditions: 50× magnification, 10 s of accumulation time, and 10 mW, 785 nm laser power.

injection-molding parameters were injection pressure 25 bar, melt temperature 240−250 °C, mold temperature 40 °C, hold time 6 s, and cool time 20 s. A detailed description of the procedure has been presented elsewhere.[15] Nanocomposite films of about 0.1 mm thickness were obtained by compression-molding at 240 °C for 2 min and subsequently quenched under constant pressure at a cooling rate of ~300 °C min^{-1}. Circular gold electrodes (20 mm in diameter) were deposited onto the surfaces of the film sample. The complex permittivity $\epsilon^* = \epsilon' - i\epsilon''$, where ϵ' represents the permittivity and ϵ'' the dielectric loss, of the nanocomposites was measured as a function of frequency (10^{-1} Hz < F < 10^7 Hz) and temperature (−150 up to 75 °C) by using a Novocontrol broadband dielectric spectrometer. Alternating current (ac) electrical conductivity was derived by $\sigma(\omega) = \epsilon_0 2\pi F\epsilon''$, where ϵ_0 is the vacuum permittivity. Small- and wide-angle X-ray scattering (SAXS and WAXS) measurements were performed at the X3A2 beamline at the National Synchrotron Source (NSLS) at Brookhaven National Laboratory. The synchrotron radiation was monochromatized to $\lambda = 0.154$ nm. SAXS and WAXS patterns were recorded using two Fuji HR-VTM imaging plates (200 × 250 mm) located at 1300 and 215 mm away from the sample, respectively. Data reduction was accomplished as described elsewhere.[16]

3. Results and Discussion

3.1. Electrical Measurements of the SWCNT−PBT Films. Parts a and b of Figure 2 show the ac conductivity, $\sigma(F)$, and the permittivity, ϵ', respectively, as a function of frequency for samples with different SWCNT concentrations. For SWCNT concentrations below 0.2 wt %, a $\sigma(F) \propto F^s$ dependence is observed, the exponent s being close to 1, which is the expected behavior for insulating materials. However, for the sample with 0.2% SWCNT $\sigma(\omega)$ is frequency independent below a critical frequency, F_c, above which it follows a $\sigma(F) \propto F^s$ dependence with $s \approx 0.75$. The frequency-independent $\sigma(F)$ is characteristic of a non-dielectric behavior with a significant direct current (dc) conductivity σ_{dc} . This last behavior fits into the so-called universal dynamic response proposed by Jonscher[3,17] and has been also reported for SWCNT−epoxy resin nanocomposites.[11] The inset of Figure 2a shows $\sigma(F)$ values taken at $F = 0.1$ Hz in order to emphasized the discontinuous increase in conductivity upon increasing the SWCNT concentration. At low SWCNT concentration the permittivity values, ϵ', remain nearly frequency

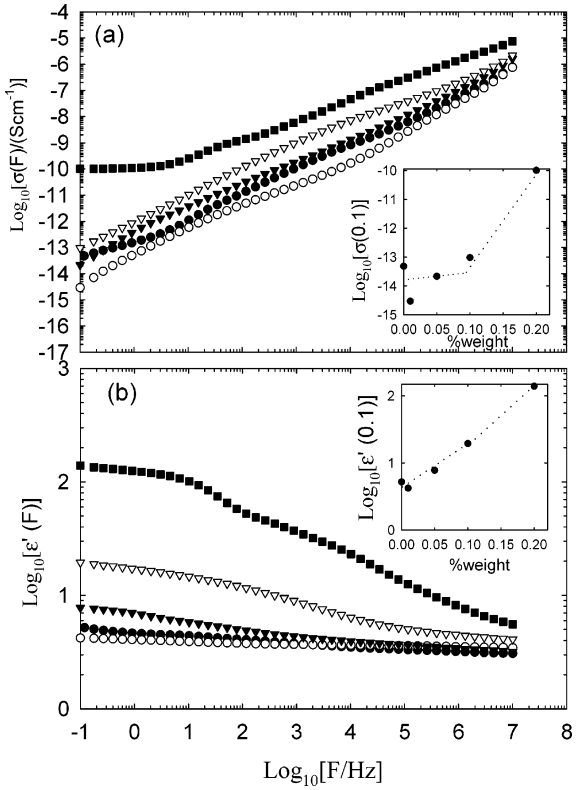

Figure 2. (a) Alternating current conductivity, $\sigma(F)$, and (b) dielectric constant, ϵ', as a function of frequency F for SWCNT−PBT nanocomposite with different SWCNT weight concentrations: (●) 0, (○) 0.01, (▼) 0.05, (△) 0.1, and (■) 0.2 wt % of SWCNT. The insets show the corresponding values at $F = 10^{-1}$ Hz as a function of the SWCNT weight concentration.

independent (Figure 2b). However, a decrease of ϵ' with frequency is observed as the SWCNT concentration increases. In particular, for the sample with 0.2% SWCNT $\epsilon'(F)$ is frequency independent below a critical frequency, above which it follows a $\epsilon'(F) \propto F^{-y}$ dependence with $y \approx 0.22$. The frequency dependence followed by both $\sigma(F)$ and $\epsilon'(F)$ is qualitatively similar to that reported recently for different CNT−polymer nanocomposites.[8,10,11] Exponent values of $s = 0.92$ for multiwall nanotube−poly(vinyl alcohol) composites were interpreted in terms of biased random walk in three dimensions.[8] In our case, a lower value of $s \approx 0.75$ is compatible with power laws derived for percolating random mixtures in which polarization effects between clusters are considered.[18] Moreover, in this case the critical exponents describing the power laws for $\sigma(F)$ and $\epsilon'(F)$ should fulfill that $s + y = 1$ near the percolation threshold.[19] This condition is almost obeyed in our case for the sample with 0.2 wt % of SWCNT. The limiting values $\epsilon'(F \rightarrow 0)$, which correspond to the static permittivity, clearly increase with increasing SWCNT concentration (see inset of Figure 2b). The behavior exhibited by both $\sigma(F)$ and $\epsilon'(F)$ at lower frequencies as a function of SWCNT concentration indicates that the sample with 0.2% is in the percolating regime; i.e., a charge transfer across a conducting SWCNT network has started to occur. To further support this argument and to evaluate the nature of this charge transfer, $\sigma(F)$ was measured as a function of temperature for the sample with 0.2% of SWCNT (Figure 3). From these measurements it can be seen that the limiting constant value conductivity values at low frequencies, σ_{dc}, exhibit a temperature activated behavior. In the inset of Figure 3 values of

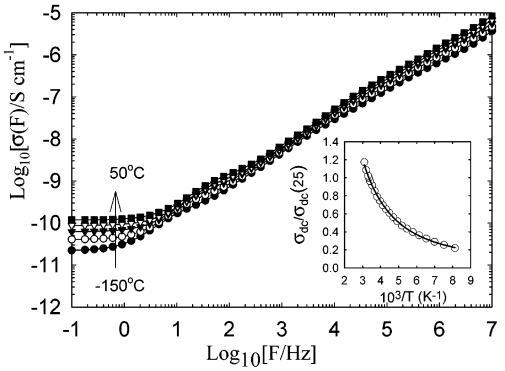

Figure 3. Alternating current conductivity, $\sigma(F)$, as a function of frequency for the nanocomposite with 0.2 wt % of SWCNT at different temperatures from −150 to 50 °C in steps of 50 °C. The inset shows the σ_{dc} obtained from the plateau at lower frequencies as a function of the reciprocal temperature. σ_{dc} has been normalized to its room temperature value.

σ_{dc}, normalized to the corresponding value at 25 °C, have been represented as a function of the reciprocal temperature. It is seen that σ_{dc} exhibits a nonlinear behavior with reciprocal temperature which qualitatively resembles that observed for carbon black composites.[1,5] This dependence of the dc electrical conductivity with temperature has been attributed to the thermal fluctuation-induced tunneling mechanism.[20] Assuming that a tunneling, activated by local temperature fluctuations,[1,20] of charge carriers from the conducting nanotubes through a potential barrier of varying height is formed in the polymer matrix the following temperature dependence of σ_{dc} is expected:

$$\sigma_{dc} \propto \exp[-T_1/(T + T_0)] \qquad (1)$$

where T_1 is related to the energy required for a charge carrier to overcome the insulator gap and T_0 is the temperature around which thermal fluctuations are significant.[1,20] A reasonable description of the data for the 0.2% of SWCNT is obtained by this model as shown by the continuous line in the inset of Figure 3 using the values of $T_0 = 225$ K and $T_1 = 1545$ K.

Results from the electrical measurements indicate that for the system SWCNT−PBT prepared in this study a relatively low concentration threshold in the proximity of 0.2% in weight of SWCNT is confirmed. This value is lower than the values previously reported in CNT nanocomposites with thermoplastic matrices and approaches those observed with thermosets.

3.2. SAXS/WAXS of the SWCNT−PBT Samples. As previously reported,[9] the onset of the conductivity in CNT nanocomposites is not a purely geometrical problem, but it is closely related to the aggregation level of the conducting nanotubes. Agglomeration of nanotubes, rather than a simple random arrangement, appears to improve efficiency of the conducting network.[9] In our case, PBT is a semicrystalline polymer with the characteristic nanostructure consisting of an alternation of crystalline lamellae and amorphous layers.[21] The semicrystalline nature of our SWCNT−PBT nanocomposites is revealed by the WAXS and SAXS patterns presented in Figure 4a,b for both PBT and the 0.2 wt % SWCNT−PBT nanocomposites for the different stages of sample processing including the extruded (E), injection-molded (IM), and film (F) samples. All samples exhibit scattering maxima in the SAXS region at a characteristic s value of semicrystalline polymers,[22]

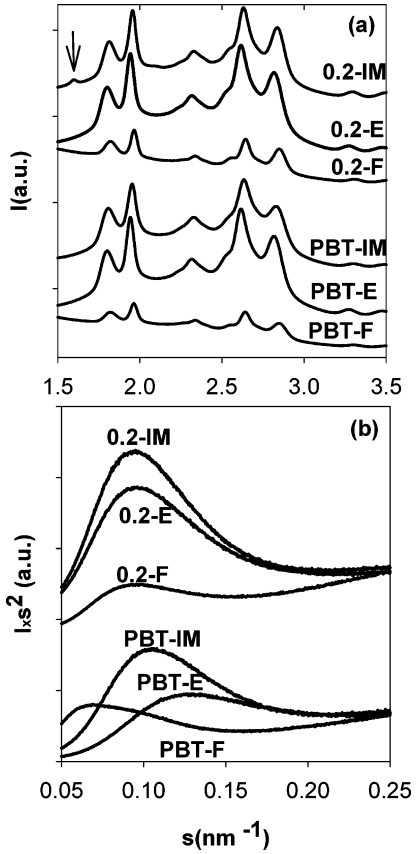

Figure 4. (a) Wide-angle X-ray scattering intensity and (b) small-angle X-ray scattering intensity, in arbitrary units, as a function of the reciprocal lattice vector, $s = (2/\lambda)\sin(\theta)$, 2θ being the scattering angle. PBT in the different stages of sample processing includes the extruded (PBT-E), injection-molded (PBT-IM), and film (PBT-F). SWCNT−PBT nanocomposite with 0.2 wt % of SWCNT: extruded (0.2-E), injection-molded (0.2-IM), and film (0.2-F). The arrow in the WAXS pattern of the 0.2-IM sample indicates the reflection attributed to a SWCNT crystal phase (see text).

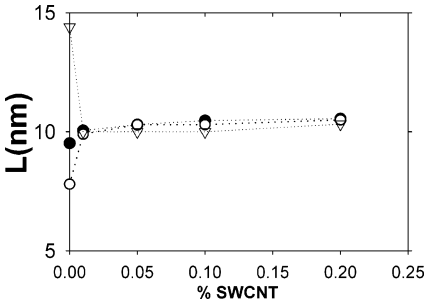

Figure 5. Variation of the long period, L, with the SWCNT weight concentration for SWCNT−PBT nanocomposite for the different stages of sample processing including the (○) extruded (E), (●) injection-molded (IM), and (▽) film (F) samples.

referred to as long spacing. The reciprocal of this s value is related to the average distance between the adjacent crystal lamellae.[22] The different scattering maxima for the PBT homopolymer reflect the different nature of the sample at the different processing stages. Figure 5 shows the dependence of the long spacing (L) with the SWCNT concentration. The equivalent long period values observed for all the SWCNT−PBT specimens can be attributed the a nucleation enhancement caused by the nanotubes.[23] The WAXS diffraction pattern for PBT corresponds to the α crystalline phase.[21] The WAXS patterns (Figure 4a) indicate that the

nanotubes do not perturb the nature of the PBT crystals. It is noteworthy the weak reflection appearing at 1.6 nm^{-1} for the 0.2 wt % IM sample. The corresponding spacing of this reflection corresponds to about 0.625 nm. Because of the fact that this reflection appears at a significantly lower angle than the characteristic 002 reflection in graphite,[24] we can attribute it to the formation of ordered agglomerates of the nanotubes during the injection process. In fact, the RBM peak observed in Figure 1 around 397 cm^{-1} reveals the existence of a population of SWCNT's around 0.62 nm, which may become crystalline ordered during injection. This reflection, only observed in the IM sample, is position dependent. A microfocus X-ray and Raman study is currently in progress. During film formation, this reflection disappears, indicating a disruption of the ordered agglomerates but not necessarily the destruction of them.

Conclusions

In conclusion, the intense dispersion process by ultrasonication and by ultrahigh-speed stirring of single wall nanotubes (SWCNT) in 1,4-butanediol and the subsequent in situ polycondensation process has made possible to prepare nanocomposites in which the percolation threshold for conductivity is around 0.2% in weight of SWCNT. This relatively low value becomes rather close to those reported for CNT nanocomposites based on thermoset polymers. On the basis of the structural measurements, we interpret that agglomeration effect of SWCNT's may lead to an enhancement for the formation of the conducting network.

Acknowledgment. This investigation has been performed under the auspices of the CNT-NET (GTC1-2000-28052) and MERG-CT-2004-505674 from the UE. The authors thank the financial support from the MCYT (Grant FPA2001-2139), Spain, for generous support of this investigation. The US group thanks the financial support by an NSF Inter-American grant (DMR0302809). Fruitful comments from I. A. Kinloch and J. S. Young during the CNT-NET meeting in Budapest (March 25−26, 2004) are greatly appreciated.

References and Notes

(1) *Carbon Black Polymer Composites*; Sichel, E. K., Ed.; Marcel Dekker: New York, 1982.
(2) Gul, V. E. *Structure and Properties of Conducting Polymer Composites*; VSP BV: Utrecht, Tokyo, 1996.
(3) *A Broadband Dielectric Spectroscopy*; Kremer, F., Schönhals, A., Eds.; Springer: Berlin, 2002.
(4) Stauffer, D. *Introduction to Percolation Theory*; Taylor & Francis: London, 1985.
(5) Connor, M. T.; Roy, S.; Ezquerra, T. A.; Baltá-Calleja, F. J. *Phys. Rev. B* **1998**, *57*, 2286.
(6) Flandin, L.; Prasse, T.; Schueler, R.; Schulte, K.; Bauhofer, W.; Cavaille, J. Y. *Phys. Rev. B* **1999**, *59*, 14349.
(7) Jäger, K. M.; McQueen, D. H.; Tchmutin, I. A.; Ryvkina, N. G.; Klüppel, M. *J. Phys. D: Appl. Phys.* **2001**, *34*, 2699.
(8) Kilbribe, B. E.; Coleman, J. N.; Fraysse, J.; Fournet, P.; Cadek, M.; Drury, A.; Hutzler, S.; Roth, S.; Blau, W. J. *J. Appl. Phys.* **2002**, *92*, 4024.
(9) Sandler, J. K. W.; Kirk, J. E.; Kinloch, I. A.; Shaffer, M. S. P.; Windle, A. H. *Polymer* **2003**, *44*, 5893.
(10) Pötschke, P.; Dudkin, S. M.; Alig, I. *Polymer* **2003**, *44*, 5023.
(11) Barrau, S.; Demont, P.; Peigney, A.; Laurent, C.; Lacabanne, C. *Macromolecules* **2003**, *36*, 5187.
(12) Gong, X.; Liu, J.; Baskaran, S.; Voise, R. D.; Young, J. S. *Chem. Mater.* **2000**, *12*, 1049.
(13) Pötschke, P.; Bhattacharyya, A. R.; Janke, A. *Polymer* **2003**, *44*, 8061.
(14) Lucas, M.; Young, R. J. *Phys. Rev. B* **2004**, 85405.
(15) Roslaniec, Z.; Broza, G.; Schulte, K. *Composite Interface* **2003**, *10*, 95.
(16) Nogales, A.; Sics, I.; Ezquerra, T. A.; Denchev, Z.; Baltá-Calleja, F. J.; Hsiao, B. S. *Macromolecules* **2003**, *36*, 4827.
(17) Jonscher, A. K. *Nature (London)* **1977**, *267*, 673.
(18) Song, Y.; Noh, T. W.; Lee, S.; Gaines, J. R. *Phys. Rev. B* **1986**, *33*, 904.
(19) Bergman, D. J.; Imry, Y. *Phys. Rev. Lett.* **1977**, *39*, 1222.
(20) Sheng, P. *Phys. Rev. B* **1980**, *21*, 2180.
(21) Alvarez, C.; Capitán, M.; Alizadeh, A.; Roslaniec, Z.; Ezquerra, T. A. *Macromol. Chem. Phys.* **2002**, *203*, 556.
(22) Strobl, G. *The Physics of Polymers*; Springer: Berlin, 1996.
(23) Valentini, L.; Biagiotti, J.; Kenny, J. M.; Santucci, S. *J. Appl. Polym. Sci.* **2003**, *87*, 708.
(24) Dziemianowicz, T.; Leong, K.; Carl, D. *Synth. Met.* **1983**, *5*, 77.

MA049440R